PBC-13-0751.R2(24833)

Genome-Wide Analysis of DNA Copy Number Alterations and Loss of Heterozygosity in Intracranial Germ Cell Tumors

Keita Terashima, MD,[1]* Alexander Yu, BS,[1] Wing-Yuk T. Chow, PhD,[1] Wei-chun J. Hsu, MD,[1] Peikai Chen, PhD,[2] Stephen Wong, PhD,[3] Yeung Sam Hung, PhD,[2] Tomonari Suzuki, MD, PhD,[4] Ryo Nishikawa, MD, PhD,[4] Masao Matsutani, MD, PhD,[4] Hideo Nakamura, MD, PhD,[5] Ho-Keung Ng, MD,[6] Jeffrey C. Allen, MD,[7] Kenneth D. Aldape, MD,[8] Jack M. Su, MD,[1] Adekunle M. Adesina, MD, PhD,[9] Hon-chiu E. Leung, PhD,[1] Tsz-Kwong Man, PhD,[1] and Ching C. Lau, MD, PhD[1]

Backgrounds. Intracranial germ cell tumors (GCTs) are rare and heterogeneous with very little is known about their pathogenesis and underlying genetic abnormalities. ***Procedures.*** In order to identify candidate genes and pathways which are involved in the pathogenesis of these tumors, we have profiled 62 intracranial GCTs for DNA copy number alterations (CNAs) and loss of heterozygosity (LOH) by using single nucleotide polymorphism (SNP) array and quantitative real time PCR (qPCR). ***Results.*** Initially 27 cases of tumor tissues with matched blood samples were fully analyzed by SNP microarray and qPCR. Statistical analysis using the genomic identification of significant targets in cancer (GISTIC) tool identified 10 regions of significant copy number gain and 11 regions of significant copy number loss. While overall pattern of genomic aberration was similar between germinoma and nongerminomatous germ cell tumors (NGGCTs), a few subtype-specific peak regions were identified. Analysis by SNP array and qPCR was replicated using an independent cohort of 35 cases. ***Conclusions.*** Frequent aberrations of *CCND2* (12p13) and *RB1* (13q14) suggest that Cyclin/CDK-RB-E2F pathway might play a critical role in the pathogenesis of intracranial GCTs. Frequent gain of *PRDM14* (8q13) implies that transcriptional regulation of primordial germ cell specification might be an important factor in the development of this tumor. Pediatr Blood Cancer 2013;9999:1–8. © 2013 Wiley Periodicals, Inc.

Key words: DNA copy number; genomic profiling; intracranial germ cell tumor; loss of heterozygosity; SNP microarray

INTRODUCTION

Intracranial germ cell tumors (GCTs) are a group of rare heterogeneous pediatric brain tumors, which show clinical and histological similarities to the more common GCTs such as ovarian or testicular tumors. Most intracranial GCTs occur at the pineal and suprasellar regions near the third ventricle and mainly affect male adolescents and young adults. Although the survival rate of pure germinoma is excellent (approximately 90% overall survival), optimal volume and dose of radiation and the role of chemotherapy is not clear [1–4]. In contrast, the outcome of nongerminomatous germ cell tumors (NGGCTs), a heterogeneous group including teratoma, yolk sac tumor, choriocarcinoma, and embryonal carcinoma, is poor (approximately 60% overall survival) and the standard treatment for NGGCTs remains controversial [2,5–8]. Since the treatment of intracranial GCTs is different depending on the subtype, accurate subclassification of these tumors is critically important.

The anatomic location of most intracranial GCTs makes their surgical management very challenging. Currently, stereotactic or endoscopic biopsy is the mainstay for diagnosing intracranial GCTs and some NGGCTs can be diagnosed without biopsy based on tumor markers in serum and cerebrospinal fluid (CSF): alpha fetoprotein (AFP) and/or beta human chorionic gonadotropin (βHCG). However, NGGCT is quite a heterogeneous group of tumors often mixed with multiple subtypes and their clinical behavior is unpredictable. Thus novel genetic signatures which can complement conventional methods of subclassification and risk stratification are needed. While surgical resection, radiation therapy and chemotherapy can be effective, these conventional modalities also have high morbidity associated with them [3,9]. Therefore, the discovery of novel targeted therapy is essential to further improve the outcome of patients with intracranial GCTs.

Because of the scarcity of tissue samples available, very little basic research had been carried out and the biology of intracranial GCTs is poorly understood. For example, the cell of origin of intracranial GCTs is still controversial and the molecular mechanism of tumorigenesis remains elusive. Cytogenetic and molecular data of intracranial GCTs are sparse with only a handful

DOI 10.1002/pbc.24833
Published online in Wiley Online Library (wileyonlinelibrary.com).

Additional Supporting Information may be found in the online version of this article at the publisher's web-site.

[1]Department of Pediatrics, Texas Children's Cancer and Hematology Centers, Baylor College of Medicine, Houston, Texas; [2]Department of Electrical and Electronic Engineering, University of Hong Kong, Pokfulum, Hong Kong; [3]Department of Systems Medicine and Bioengineering, The Methodist Hospital Research Institute, Houston, Texas; [4]Department of Neurosurgery, Saitama Medical University, Hidaka, Saitama, Japan; [5]Department of Neurosurgery, Kumamoto University, Kumamoto, Japan; [6]Department of Pathology, Chinese University of Hong Kong, Shatin, New Territories, Hong Kong; [7]Department of Pediatric Neuro-oncology, New York University Langone Medical Center and School of Medicine, New York, New York; [8]Department of Pathology, The University of Texas MD Anderson Cancer Center, Houston, Texas; [9]Department of Pathology and Immunology, Baylor College of Medicine, Houston, Texas; Children's Cancer Center, National Center for Child Health and Development, 2-10-1 Okura, Setagaya, Tokyo 157-8535, Japan

Grant sponsor: This work was, in part, supported by the Children's Brain Tumor Foundation; Grant sponsor: The Gillson Longenbaugh Foundation; Grant sponsor: The Carl C. Anderson Sr. and Marie Jo Anderson Charitable Foundation; Grant sponsor: Cancer Fighters of Houston; Grant sponsor: Toyota-JMSA Scholarship; Grant sponsor: St. Baldrick's Foundation

Conflict of interest: Nothing to declare.

*Correspondence to: Ching C. Lau, Texas Children's Hospital, 1102 Bates St., Feigin Center, Suite C.1030.11, Houston, TX 77030.
E-mail: cclau@txch.org

Received 19 August 2013; Accepted 1 October 2013

of reports on the cytogenetic analysis available [10,11]. Results of comparative genomic hybridizations (CGH) and single nucleotide polymorphism (SNP) microarrays of intracranial GCTs in smaller series have been reported [12–14]. Presently, no convincing evidence implicating the involvement of particular genes or pathways in the tumorigenesis of intracranial GCTs has been identified.

To comprehensively analyze the genome-wide CNAs and loss of heterozygosity (LOH) of intracranial GCTs, we have studied a series of 62 intracranial GCTs by using high-density oligonucleotide SNP array and quantitative real time PCR (qPCR). This study was conducted as an international collaboration of six institutions to overcome the obstacle of tissue scarcity.

MATERIALS AND METHODS

Samples

Sixty-two cases from six institutions were enrolled through local Institutional Review Board-approved protocols after written informed consents were obtained. All tumor tissues and peripheral blood were collected at the time of initial surgery prior to any adjuvant treatment and were snap frozen in liquid nitrogen and stored at −80˚C until the time of DNA extraction. Diagnosis was made at each local institution based on clinical, laboratory and histopathologic evaluation. Initially 27 cases with both tumor tissues and matched blood samples were analyzed by SNP array and the results were validated by qPCR method. Then SNP array data of 21 cases without matched control were analyzed independently using pooled blood controls. Likewise, qPCR study was replicated with 25 cases 11 of which also have SNP array data from the second cohort (Table I). Thus a total of 35 independent cases were used in the validation by either SNP array or qPCR.

DNA Extraction and SNP Microarray Hybridization

Genomic DNA was extracted from each tumor sample by QIAamp DNA Mini Kit (Qiagen, Valencia, CA) and blood sample by Wizard Genomic DNA Purification Kit (Promega, Madison, WI) according to the manufacturers' protocols and quantified by spectrophotometry (Nanodrop, Wilmington, DE) with quality checked on 1% agarose gel. SNP array profiling was performed using Affymetrix GeneChip Human Mapping 100K Arrays (Hind III array) and a GeneChip Scanner 3000 (Affymetrix, Inc., Santa Clara, CA). Data processing was done using the Affymetrix GCOS and GDAS software according to the manufacturer's instructions. Samples were excluded from further analysis if the call rate was less than 90%, the outlier rate was more than 5% or hierarchical tree showed distinct clustering.

Copy Number and LOH Analysis

CEL files produced by GCOS software for the qualified arrays were imported into Partek Genomic Suite (Partek, St. Louis, MO) and analyzed using the copy number analysis and LOH workflow. Signal intensity of each tumor case was compared either with paired reference blood control or pooled data of blood controls. Copy number was determined based on the signal intensity ratio between cases and controls. Significantly different regions were determined using the genomic segmentation algorithm of the Partek Genomic Suite. Each genomic region was defined as CNA when the regional copy number average was <1.5 for loss and >2.5 for gain. For LOH analysis, the probability of observing a heterozygous SNP in a region of LOH was determined using the genotype error rate. In a region without LOH, the probability of observing a heterozygous SNP was estimated using the observed frequency from the germline control samples. Homozygous SNPs in the control samples were excluded from the analysis. The frequency of CNA and copy neutral LOH were calculated for each segment based on the number of positive cases over total number of cases. Database of Genomic Variants (DGV) hosted by The Centre for Applied Genomics (http://projects.tcag.ca/variation/) was used to check germline copy number variation (CNV).

Quantitative Real-Time PCR (qPCR)

CCND2 and *NANOG* from chromosome 12p, *PRDM14* from 8q, *RB1* from 13q and *AR* from X were selected for validation in regions of CNA. Copy number of *CCND2*, *PRDM14*, and *RB1* were further validated by qPCR using the expanded cohort. Quantitative PCR by SYBR Green was performed on an ABI Prism 7900 system (Applied Biosystems, Foster City, CA). Conditions for amplification were as follows: 1 cycle at 95˚C for 10 minutes, 40 cycles at 95˚C for 30 seconds/62˚C for 1 minute/72˚C for 30 seconds, and 1 cycle at 95˚C for 1 minute/60˚C for 10 minutes (dissociation curve). All primer sequences are listed in Table SI. *B2M* and *PTCH1* genes were selected as normal internal controls for the relative quantification. Commercially available genomic DNA (Human Genomic DNA: Promega) was used as normal external control. As a positive control for X chromosome copy number gain, blood DNA sample of individuals with karyotypes 47,XXY, 48,XXX, and 49,XXXXY (Coriell Institute, Camden, NJ) were used.

Copy Number Determination by qPCR Method

Mean threshold cycle (C_t) values from triplicates for each sample were normalized by delta-delta C_t ($\Delta\Delta C_t$) method, and inferred copy number (ICN) was calculated using the formula: $ICN = 2^{(1-\Delta\Delta C_t)}$. The reference ranges for normal copy number of each gene were established by analyses of ICN of patients' blood samples. On the basis of mean ICN $\pm$ 2 SD, the reference intervals were set as, 1.48–2.55 for *CCND2*, 1.42–2.65 for *NANOG*, 1.54–2.25 for *PRDM14*, 1.75-2.61 for *RB1*, 0.63–1.53 for *AR* in male patients, and 1.58–2.32 for *AR* in female patients. ICN of X chromosome in positive controls validated the methods (1.72: 47, XXY, 2.99: 48, XXX, 4.63: 49, XXXXY).

Genomic Identification of Significant Targets in Cancer (GISTIC) Analysis

GISTIC tool [15] which takes into account both the amplitude and frequency of CNAs was used to identify statistically significant regions of CNA among overall cohort and different subgroups of intracranial GCTs. The significance of CNA at a particular genomic location is determined based on a test statistic computed using the segmentation log ratios of all samples. The threshold false discovery rate for GISTIC analysis was set at 0.05.

TABLE I. Demographics and Clinical Characteristics of All 62 Subjects

ID	Sex	Age (year)	Location	Pathological diagnosis	SNP array	qPCR
Discovery cohort						
1	F	7	Suprasellar	Germinoma	Tumor and matched blood	Performed
2	M	10	Pineal	Germinoma	Tumor and matched blood	Performed
3	M	11	Pineal + periventricular metastases	Germinoma	Tumor and matched blood	Performed
4	M	12	Left frontal lobe	Germinoma	Tumor and matched blood	Performed
5	M	15	Pineal + anterior horn	Germinoma	Tumor and matched blood	Performed
6	F	15	Suprasellar	Germinoma	Tumor and matched blood	Performed
7	F	17	Suprasellar	Germinoma	Tumor and matched blood	Performed
8	F	18	Suprasellar	Germinoma	Tumor and matched blood	Performed
9	M	22	Pineal	Germinoma	Tumor and matched blood	Performed
10	M	24	Cerebral	Germinoma	Tumor and matched blood	Performed
11	M	24	Pineal	Germinoma	Tumor and matched blood	Performed
12	M	20	Pineal	Germinoma with STGC	Tumor and matched blood	Performed
13	M	23	Basal ganglia	Germinoma with STGC	Tumor and matched blood	Performed
14	M	2	Cerebellum	Yolk sac tumor	Tumor and matched blood	Performed
15	M	12	Pineal	Yolk sac tumor	Tumor and matched blood	Performed
16	M	11	Pineal	Teratoma + yolk sac and trophoblastic elements	Tumor and matched blood	Performed
17	M	12	Basal ganglia	Germinoma + yolk sac tumor	Tumor and matched blood	Performed
18	M	24	Pineal	Yolk sac tumor + immature teratoma	Tumor and matched blood	Performed
19	F	5	Suprasellar	Immature teratoma + embryonal carcinoma + choriocarcinoma	Tumor and matched blood	Performed
20	M	14	Pineal	Germinoma + embryonal carcinoma	Tumor and matched blood	Performed
21	M	8	Pineal	Immature teratoma + germinoma	Tumor and matched blood	Performed
22	F	10	Suprasellar	Immature teratoma + germinoma	Tumor and matched blood	Performed
23	M	21	Pineal	Immature teratoma	Tumor and matched blood	Performed
24	M	4	Posterior fossa	Mature teratoma	Tumor and matched blood	Performed
25	M	10	Pineal	Germinoma + mature teratoma	Tumor and matched blood	Performed
26	F	14	Left frontal lobe	Germinoma	Tumor and matched blood	N/A
27	M	16	Basal ganglia	Germinoma	Tumor and matched blood	N/A
Replication cohort						
28	M	17	Pineal	Germinoma	Tumor only	Performed
29	M	17	Pineal + suprasellar	Germinoma	Tumor only	Performed
30	M	18	Pineal + anterior horn	Germinoma	Tumor only	Performed
31	F	24	Suprasellar	Germinoma	Tumor only	Performed
32	M	27	Pineal	Germinoma	Tumor only	Performed
33	M	14	Suprasellar	Germinoma with STGC	Tumor only	Performed
34	M	12	Pineal	Yolk sac tumor	Tumor only	Performed
35	M	13	Pineal	Immature teratoma	Tumor only	Performed
36	M	16	Pineal	Germinoma + immature teratoma	Tumor only	Performed
37	M	15	Pineal	Mature teratoma + germinoma with STGC	Tumor only	Performed
38	M	19	Pineal	Mixed germ cell tumor	Tumor only	Performed
39	M	4	Pineal	Germinoma	Tumor only	N/A
40	M	14	Pineal	Germinoma	Tumor only	N/A
41	F	18	Corpus callosum	Germinoma	Tumor only	N/A
42	M	18	Pineal	Germinoma	Tumor only	N/A
43	M	19	Pineal	Germinoma	Tumor only	N/A
44	F	25	Hypothalamus	Germinoma	Tumor only	N/A
45	M	32	Third ventricle	Germinoma	Tumor only	N/A
46	M	26	Pineal	Embryonal carcinoma	Tumor only	N/A
47	N/A	N/A	N/A	N/A	Tumor only	N/A
48	N/A	N/A	N/A	N/A	Tumor only	N/A
49	M	7	Basal ganglia	Germinoma	N/A	Performed
50	F	8	Suprasellar	Germinoma	N/A	Performed
51	M	8	Suprasellar	Germinoma	N/A	Performed
52	M	13	Pineal + suprasellar	Germinoma	N/A	Performed
53	M	16	Pineal	Germinoma	N/A	Performed
54	M	16	Basal ganglia + temporal lobe	Germinoma	N/A	Performed
55	M	25	Pineal + suprasellar	Germinoma	N/A	Performed

(*Continued*)

TABLE I. (*Continued*)

ID	Sex	Age (year)	Location	Pathological diagnosis	SNP array	qPCR
56	M	40	Pineal + basal ganglia	Germinoma	N/A	Performed
57	F	4	Suprasellar	Immature teratoma	N/A	Performed
58	M	10	Pineal	Immature teratoma	N/A	Performed
59	M	16	Pineal	Immature teratoma	N/A	Performed
60	M	10	Pineal	Germinoma + Teratoma	N/A	Performed
61	M	22	Pineal	Teratoma	N/A	Performed
62	M	0	Cerebellar	Mature teratoma	N/A	Performed

RESULTS

Copy Number and LOH Analysis by SNP Microarray

The demographic and clinical characteristics of all 62 cases are summarized in Table I. The median age of patients was 15 years (range, 8 months–40 years) and there is a male predominance (80%). Germinoma was the most common histologic subtype (63%). Tumors were most commonly located at the pineal (58%) and suprasellar (20%) regions.

After stringent quality control evaluation, 48 cases were included in the final SNP array analysis. Cases with low call rate (<90%) and high outlier rate (>5%) were excluded. These 48 cases were divided into two cohorts. Twenty seven cases of tumor tissues with matched blood samples were analyzed as a discovery set with the remaining 21 cases without matched blood DNA analyzed separately as a validation set. The tumor genomes of intracranial GCTs are often complex with multiple CNAs and LOHs in each case and virtually all cases (Fig. 1A). The size of CNAs ranged from small intrachromosomal segments to those involving entire chromosomes. Several regions of recurrent CNAs were identified. Most frequently observed copy number gains were regions on chromosomes 1q (44%), 2p (37%), 7q (37%), 8q (41%), 12p (59%), 14 (33%), 20q (30%), 21 (63%), 22 (41%), and Xq (44%). Frequently observed copy number losses were regions on chromosomes 1p (26%), 4q (26%), 5q (33%), 9q (30%), 10q (37%), 11q (41%), and 13 (48%) (Fig. 1B). Most copy number gains are of relatively low level. However, we identified 28 regions with more than five copies (mean copy number > 4.5). These regions were generally small focal segments with median size of 1.7 Mb (range: 0.1–151 Mb). They also showed a tendency to recur in some particular cases (Table II). No homozygous loss was identified. We identified two regions with recurrent copy neutral LOH at 11q (15%) and Xq (11%) (Fig. 1A).

GISTIC Analysis

Next, we used the GISTIC tool to identify the most significant regions of CNAs. Despite overall complex genomic aberration patterns with almost every region of the genome having CNA in at least one case, only 10 peak regions with gain and 11 peak regions with loss were identified using GISTIC analysis (Fig. 2A and Table SII). Some peaks occurred within background broad regions (e.g., gain of 8q13.2), but other peaks occurred focally without background broad regions (e.g., gain of 14q11.2). A total of 460 genes were identified at four focal peak regions: 8q13.2 gain, 14q11.2 gain, 22q11.22 gain, 1p36.12 loss (Table SIII).

SNP array data from germinomas and NGGCTs were also analyzed separately by GISTIC tool (Figs. 2B,C and Table SII). Most peak regions were detected in both subtypes, but a few subtype-specific peak regions emerged. Gain peaks at cytoband 2q22.2, 8q13, 7p15.1, 14q.11.2 and a loss peak at 5p14.3 were only observed in germinomas. On the other hand, a focal loss peak at 5q32 was seen only in NGGCTs.

Subsequently, we analyzed SNP array data of 21 independent cases without matched blood as a replication cohort using pooled blood controls. Though GISTIC detected more peak regions than the analysis in the discovery cohort with matched blood controls, overall profile of DNA copy number was similar (Fig. S1). Most additional peaks detected in the analysis of the replication cohort were very narrow localized peaks, suggesting germline CNV, which cannot be distinguished from somatic aberration without matched germline control DNA. Among 45 peaks which were not detected in the first cohort with matched blood controls, 37 peaks (82%) were reported in DGV as CNVs in the normal population.

Validation of SNP Microarray Results by qPCR

In order to validate the CNAs identified by SNP array analysis in the discovery cohort of 27 cases, we performed real time qPCR. *CCND2* (12p13), *NANOG* (12p13), *PRDM14* (8q13), *RB1* (13q14), and *AR* (Xq12) were selected for validation because of their location at the most commonly overlapped regions of frequent CNAs. Overall, there was a good concordance of the copy number calls between the SNP array and qPCR results; *CCND2* (12p13): 88%, *NANOG* (12p13): 83%, *PRDM14* (8q13): 75%, *RB1* (13q14): 88%, *AR* (Xq12) for male: 77%, and *AR* (Xq12) for female: 83% (Table SIV).

The copy number of *CCND2*, *PRDM14*, and *RB1* in the replication cohort of 25 cases was also quantified by qPCR method. The frequency of *CCND2* gain, *PRDM14* gain and *RB1* loss was similar to those in the discovery cohort. *CCND2* gains were more common in NGGCTs. On the other hand, *PRDM14* gain and *RB1* losses were more common in germinomas and such a trend was similarly observed as in the discovery cohort (Table SV).

DISCUSSION

We report here the largest study of genome-wide copy number and LOH analysis of intracranial GCTs by SNP array. We detected genomic aberrations with higher sensitivity and definition than previous reports by chromosomal CGH method. In contrary to testicular GCTs, in which genomic aberration has been extensively

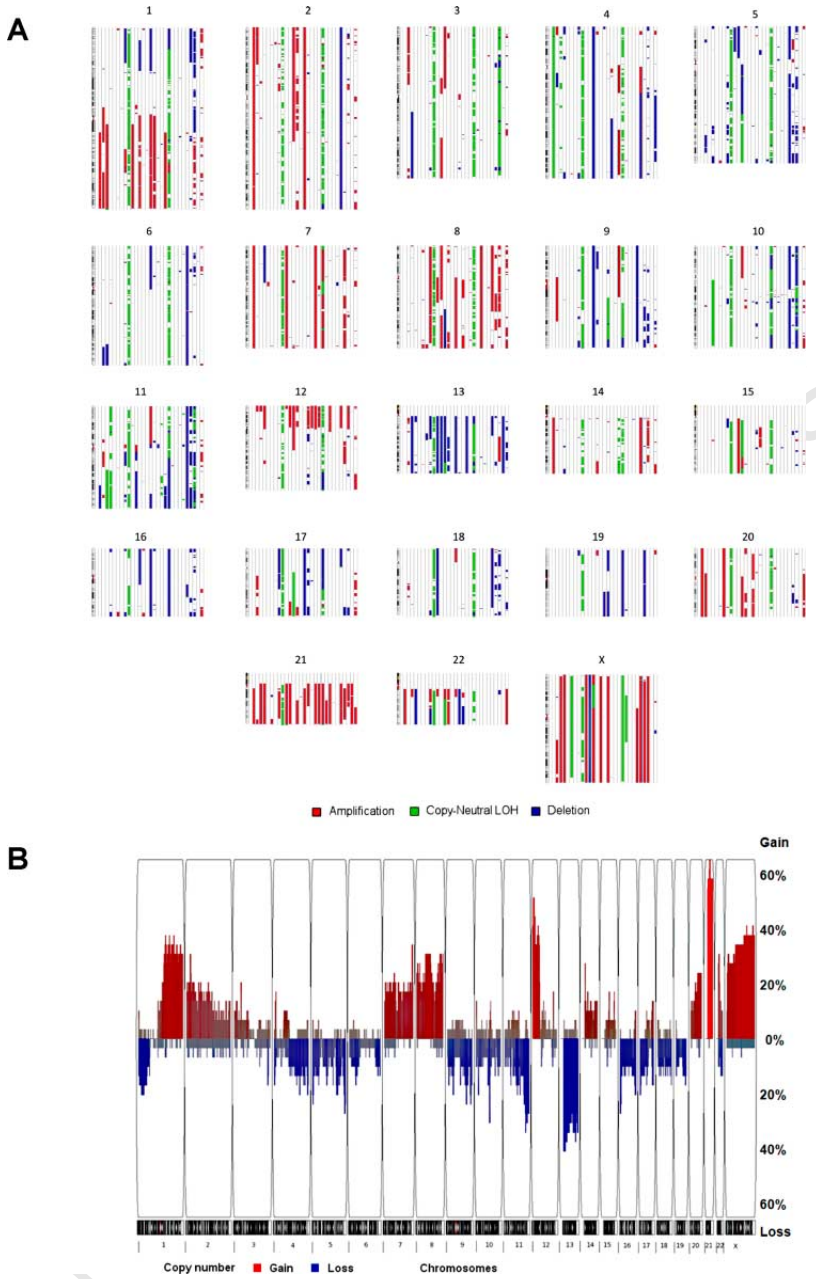

Fig. 1. DNA copy number and LOH profile of the discovery cohort. **A**: genome-wide copy number and LOH profiles of 27 intracranial GCTs were analyzed by SNP microarray. Red, green, and blue indicate gain, copy-number neutral LOH, and loss of genomic regions of each chromosome, respectively. **B**: summary of copy number aberration profiles of 27 intracranial GCTs. The frequency of copy number gain (red) and loss (blue) of genomic regions based on SNP microarray analysis are plotted and arranged according to the chromosome order along the x-axis.

studied, only two small series (15 and 19 cases, respectively) of conventional CGH analysis and one series (15 cases) of SNP array CNA analysis of intracranial GCTs are available [12–14]. Our series is larger and includes 62 cases with 27 matched blood control samples. Our analysis detected most recurrent genomic aberrations which were previously reported in intracranial GCTs but with more refined boundaries. In addition, we were able to detect novel small focal regions of genomic aberration and copy neutral LOH. The DNA copy number calls by SNP array and Partek Genomic Suite were validated by qPCR method. Concordance rates of four representative loci were 75–88%. There is a trend that qPCR would call normal in a minority of cases which SNP array called abnormal. This could be due to the relatively wide normal range calculated from the data from blood samples, which could contain rare germline CNVs within the PCR amplicons.

TABLE II. Genomic Regions With More Than Five DNA Copies

ID	Mean copy number	Cytoband
26	5.3	1p36.33-p36.32
26	4.6	1q12
27	5.1–5.7	1q25.3-q41
9	4.6	4q12
16	5.7	4q13.1
18	5.1–5.9	7q36.2-q36.3
7	4.9–16.3	8q11.21-q13.3
16	6.3	8q12.1
8	4.9	8q24.23
8	6.3	11p11.12-q11
18	7.9	11q11
15	4.6–8.8	12p13.2-p11.1
20	6.2	12p11.22
16	4.6–7.5	12q12.33-q11
18	5.8	12q14.1-q21.1
7	7.2	14q11.2
1	5.1	14q11.2
16	4.5	14q13.1
27	5.8	21q21.1-21.2
8	4.9	21q21.1-21.2
20	4.5	21q21.1-q21.2
30	4.6–4.8	21q21.1-q22.3
1	5.0	21q22.3
26	5.0	21q22.3
12	5.3	22q11.21-q11.22
3	4.6	22q11.21-q11.23
26	5.2	22q13.31
15	4.6	Xp22.33-q28
27	4.9	Xq27.2-q26

GISTIC identified distinct focal peak regions such as 8q13.2 gain. These peak regions are small enough to have all the genes identified within these regions. The 8q13.2 region contains *PRDM14* gene, a PR-domain containing transcription factor. We identified a gain peak which encompasses *PRDM14* in 13 out of 27 cases (48%), eight of which were germinoma cases. *PRDM14* is one of the key transcriptional regulators of primordial germ cell (PGC) specification and over-expression of *PRDM14* has been reported in other cancers [16–19]. Recently a genome wide association study of testicular GCT using SNP array also identified PRDM14 as a susceptibility locus [20]. These data suggest that *PRDM14* might play a pivotal role in the tumorigenesis of intracranial GCTs, especially in germinoma.

The overall pattern of genomic aberrations in intracranial GCTs in our series is very similar to those of two earlier studies using array CGH [12,13], but significantly different from those of a more recent study by Wang et al. which also utilized high-resolution SNP arrays [12–14]. Their results of 15 intracranial GCTs showed recurrent copy number losses such as 4q, 9q, and 13, which were similar to our findings, but identified only one region of recurrent copy number gain found on chromosome 21. The significant difference between various studies may be due to the difference of assay platforms or ethnic background of the subjects in each study.

While the overall pattern of genomic aberration was similar between germinoma and NGGCTs, a few subtype-specific peak regions (2q22.2, 5p14.3, 5q32, 8q13, 7p15.1, 14q.11.2) were identified for the first time. Compared to frequent CNAs, copy neutral LOH was relatively rare in intracranial GCTs. One of the regions of recurrent copy neutral LOH was identified in 11q where copy number loss was also frequently observed and GISTIC analysis identified a broad peak region at 11q23.

Frequent gain of chromosome 12p has been reported previously in intracranial GCTs. The characteristic isochromosome 12p found in testicular GCTs has also been found in intracranial GCTs, but majority of 12p gains in intracranial GCTs are either whole 12p arm gain or with various other complex structural abnormalities [10]. In the current series, the most significant GISTIC region was 12p13 where multiple candidate genes, such as *CCND2*, *KRAS*, *NANOG*, and *DPPA3* (*STELLA*) are located. Gain of the *CCND2* gene copy was detected in 14 out of 27 cases (52%) and gain of *KRAS* was detected in 13 out of 27 cases (48%). *KRAS* is one of the most frequently mutated oncogenes in a variety of human cancers and *CCND2* is involved in the inactivation of the tumor suppressing activity of *RB1* by phosphorylation [21]. Concordant increase in copy number and expression of *KRAS* and *CCND2* has been observed in testicular GCTs [22]. Recently, Lee et al. [23] showed malignant transformation of murine spermatogonial stem cells (SSC) by transfecting *Ras* and *Ccnd2* to this small pool of self-renewing stem cells in the earliest stage in spermatogenesis. We sequenced *KRAS* by using remaining DNA in 21 cases and detected point mutations in two cases (data not shown). Both *NANOG* and *DPPA3* are key genes in germ cell development, specifically in the development of PGC [24]. Expression of both proteins in GCTs has also been reported previously [25,26].

The most frequently observed copy number loss was chromosome 13 with the most significant GISTIC peak region at 13q12 which contains *RB1*. Copy number loss and LOH of *RB1* gene was detected in 13 out of 27 cases (48%) consistent with previous reports of LOH of *RB1* in testicular GCTs [27]. Frequent aberration of *CCND2* and *RB1* suggests that Cyclin/CDK-RB-E2F pathway might play a critical role in the pathogenesis of intracranial GCTs [28]. Copy number abnormalities of multiple key genes in this pathway such as *CDK4*, *CDK6*, and *CDKN2A* were also observed in our series, while we did not detect recurrent mutation of these genes in those 21 cases we investigated (data not shown). Cyclin/CDK-RB-E2F pathway has been suggested as an important pathway for initiation and development of malignant germ cells in testicular GCTs [22].

Gain of X chromosome has been observed in GCTs, including intracranial GCTs [29]. We observed frequent X chromosome gains exclusively in male patients. Schneider et al. [13] reported similar result of frequent X chromosome gain in male patients and the incidence of intracranial GCT is higher in individuals with Klinefelter syndrome (XXY) [30]. Therefore, X chromosome gain is likely to be critical in the development of intracranial GCTs [10,30].

In conclusion, we report the largest series of genome-wide CNA and LOH profiles of intracranial GCTs and describe the pattern of genomic aberration. By using GISTIC analysis, statistically significant regions of CNAs, including subtype-specific CNAs were discovered. Frequent aberration of *CCND2* and *RB1* suggests that Cyclin/CDK-RB-E2F pathway might play a critical role in the pathogenesis of intracranial GCTs. Frequent gain of *PRDM14* imply that transcriptional regulation of PGC specification might be an important function in the biology of this tumor.

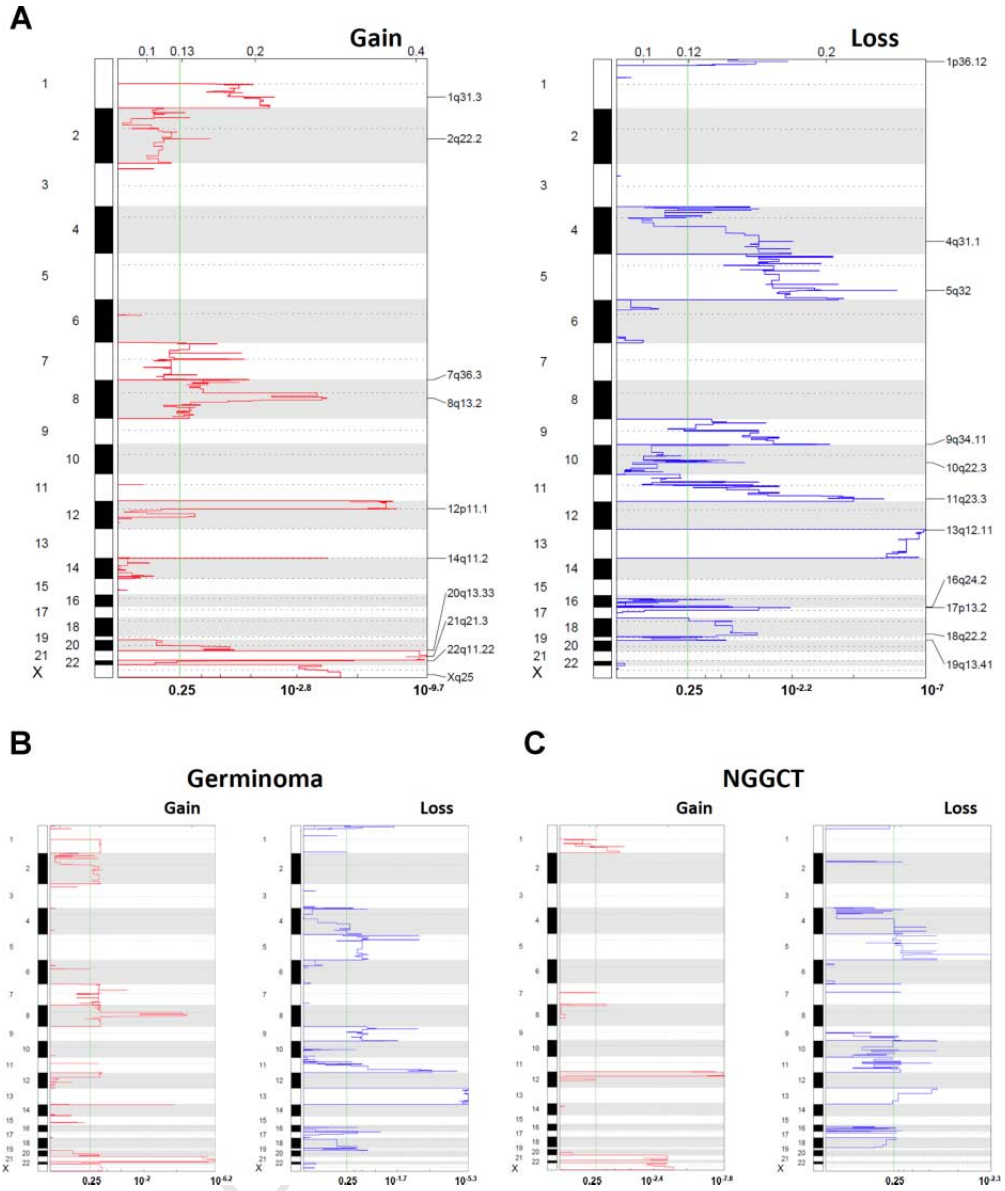

Fig. 2. GISTIC analysis of copy number aberration in the discovery cohort. The statistical significance of the aberrations is displayed as FDR q values to correct for multiple-hypothesis testing. Chromosome positions are indicated along the y-axis with centromere positions indicated by dotted lines. Red plot indicates gain events and blue plot indicates loss events. **A**: All 27 intracranial GCT cases. Ten peak regions with gain and 11 peak regions with loss are identified. **B**: GISTIC analysis of 15 germinoma cases. **C**: GISTIC analysis of 12 NGGCT cases.

REFERENCES

1. Fujimaki T. Central nervous system germ cell tumors: Classification, clinical features, and treatment with a historical overview. J Child Neurol 2009;24:1439–1445.
2. Matsutani M. Pineal germ cell tumors. Prog Neurol Surg 2009;23:76–85.
3. Aoyama H, Shirato H, Ikeda J, et al. Induction chemotherapy followed by low-dose involved-field radiotherapy for intracranial germ cell tumors. J Clin Oncol 2002;20:857–865.
4. Calaminus G, Kortmann R, Worch J, et al. SIOP CNS GCT 96: Final report of outcome of a prospective, multinational nonrandomized trial for children and adults with intracranial germinoma, comparing craniospinal irradiation alone with chemotherapy followed by focal primary site irradiation for patients with localized disease. Neuro Oncol 2013;15:788–796.
5. Packer RJ, Cohen BH, Cooney K. Intracranial germ cell tumors. Oncologist 2000;5:312–320.
6. Echevarria ME, Fangusaro J, Goldman S., Pediatric central nervous system germ cell tumors: A review. Oncologist 2008;13:690–699.
7. Sawamura Y, Ikeda J, Shirato H, et al. Germ cell tumours of the central nervous system: Treatment consideration based on 111 cases and their long-term clinical outcomes. Eur J Cancer 1998;34:104–110.
8. Matsutani M, Sano K, Takakura K, et al. Primary intracranial germ cell tumors: A clinical analysis of 153 histologically verified cases. J Neurosurg 1997;86:446–455.
9. Fouladi M, Grant R, Baruchel S, et al. Comparison of survival outcomes in patients with intracranial germinomas treated with radiation alone versus reduced-dose radiation and chemotherapy. Childs Nerv Syst 1998;14:596–601.
10. Biegel JA. Cytogenetics and molecular genetics of childhood brain tumors. Neuro Oncol 1999;1:139–151.
11. Bhattacharjee MB, Armstrong DD, Vogel H, et al. Cytogenetic analysis of 120 primary pediatric brain tumors and literature review. Cancer Genet Cytogenet 1997;97:39–53.
12. Rickert CH, Simon R, Bergmann M, et al. Comparative genomic hybridization in pineal germ cell tumors. J Neuropathol Exp Neurol 2000;59:815–821.
13. Schneider DT, Zahn S, Sievers S, et al. Molecular genetic analysis of central nervous system germ cell tumors with comparative genomic hybridization. Mod Pathol 2006;19:864–873.
14. Wang HW, Wu YH, Hsieh JY, et al. Pediatric primary central nervous system germ cell tumors of different prognosis groups show characteristic miRNome traits and chromosome copy number variations. BMC Genomics 2010;11:132.
15. Beroukhim R, Getz G, Nghiemphu L, et al. Assessing the significance of chromosomal aberrations in cancer: Methodology and application to glioma. Proc Natl Acad Sci USA 2007;104:20007–20012.
16. Dettman EJ, Simko SJ, Ayanga B, et al. Prdm14 initiates lymphoblastic leukemia after expanding a population of cells resembling common lymphoid progenitors. Oncogene 2011;30:2859–2873.
17. Dettman EJ, Justice MJ. The zinc finger SET domain gene Prdm14 is overexpressed in lymphoblastic lymphomas with retroviral insertions at Evi32. PLoS ONE 2008;3:e3823.

18. Yamaji M, Seki Y, Kurimoto K, et al. Critical function of Prdm14 for the establishment of the germ cell lineage in mice. Nat Genet 2008;40:1016–1022.
19. Nishikawa N, Toyota M, Suzuki H, et al. Gene amplification and overexpression of PRDM14 in breast cancers. Cancer Res 2007;67:9649–9657.
20. Ruark E, Seal S, McDonald H, et al. Identification of nine new susceptibility loci for testicular cancer, including variants near DAZL and PRDM14. Nat Genet 2013;45:686–689.
21. Kranenburg O. The KRAS oncogene: Past, present, and future. Biochim Biophys Acta 2005;1756:81–82.
22. von Eyben FE. Chromosomes, genes, and development of testicular germ cell tumors. Cancer Genet Cytogenet 2004;151:93–138.
23. Lee J, Kanatsu-Shinohara M, Morimoto H, et al. Genetic reconstruction of mouse spermatogonial stem cell self-renewal in vitro by Ras-cyclin D2 activation. Cell Stem Cell 2009;5:76–86.
24. Kurimoto K, Yamaji M, Seki Y, et al. Specification of the germ cell lineage in mice: A process orchestrated by the PR-domain proteins, Blimp1 and Prdm14. Cell Cycle 2008;7:3514–3518.
25. Santagata S, Hornick JL, Ligon KL. Comparative analysis of germ cell transcription factors in CNS germinoma reveals diagnostic utility of NANOG. Am J Surg Pathol 2006;30:1613–1618.
26. Ezeh UI, Turek PJ, Reijo RA, et al. Human embryonic stem cell genes OCT4, NANOG, STELLAR, and GDF3 are expressed in both seminoma and breast carcinoma. Cancer 2005;104:2255–2265.
27. Murty VV, Bosl GJ, Houldsworth J, et al. Allelic loss and somatic differentiation in human male germ cell tumors. Oncogene 1994;9:2245–2251.
28. Nevins JR. The Rb/E2F pathway and cancer. Hum Mol Genet 2001;10:699–703.
29. Yu IT, Griffin CA, Phillips PC, et al. Numerical sex chromosomal abnormalities in pineal teratomas by cytogenetic analysis and fluorescence in situ hybridization. Lab Invest 1995;72:419–423.
30. Arens R, Marcus D, Engelberg S, et al. Cerebral germinomas and Klinefelter syndrome. A review. Cancer 1988;61:1228–1231.